BMB
Reports

BMB Rep. 2015; 48(1): 19-24
www.bmbreports.org

Proteomic analysis of differentially expressed skin proteins in *iRhom2*^{Uncv} mice

Bing Liu, Yuan Xu, Wen-Long Li & Lin Zeng**
Institute of JingFeng Medical Laboratory Animal, 20 Dongdajie, Fengtai, Beijing 100071, China

A mouse homozygous for the spontaneous mutation *uncovered* (*Uncv*) has a hairless phenotype. A 309-bp non-frameshift deletion mutation in the N-terminal cytoplasmic domain of iRhom2 was identified in Uncv mice (*iRhom2*^{Uncv}) using target region sequencing. The detailed molecular basis for how the *iRhom2* mutation causes the hairless phenotype observed in the homozygous *iRhom2*^{Uncv} mouse remains unknown. To identify differentially expressed proteins in the skin of wild-type and homozygous *iRhom2*^{Uncv} littermates at postnatal day 5, proteomic approaches, including two-dimensional gel electrophoresis and mass spectrometry were used. Twelve proteins were differentially expressed in the skin in a comparison between wild-type and homozygous *iRhom2*^{Uncv} mice. A selection of the proteomic results were tested and verified using qRT-PCR, western blot and immunohistochemistry. These data indicate that differentially expressed proteins, especially KRT73, MEMO1 and Coro-1, might participate in the mechanism by which iRhom2 regulates the development of murine skin. [BMB Reports 2015; 48(1): 19-24]

INTRODUCTION

Our previous studies demonstrated that homozygous *Uncv* mice (MGI: 1261908) with a spontaneous mutation in the BALB/c genetic background present a hairless phenotype, inherited through an autosomal monogene (1). Genetic linkage analysis revealed that the *Uncv* gene was mapped to a 1.4-cM interval between markers D11Mit337 and D11Mit338 on mouse chromosome 11 (2). Using target region sequencing, a 309-bp non-frameshift deletion mutation was identified in the N-terminal cytoplasmic domain of iRhom2 in *Uncv* mice (*iRhom2*^{Uncv}) (unpublished data). However, the detailed molecular events by which the *iRhom2* mutation causes the hairless phenotype of the homozygous *Uncv* mouse (*iRhom2*^{Uncv}) remains unknown.

The skin, which consists of hair follicles, interfollicular epidermis, and sebaceous glands, is the largest organ of the body and provides an essential, protective barrier against body fluid loss and microbes (3). In response to specific signals from adjacent epithelial and mesenchymal cells, ectodermal cells form hair follicle buds, thereby promoting condensing of the underlying mesenchymal cells. The hair bud proliferates to form a large bulb (matrix) that further differentiates into the hair shaft, which is surrounded by the outer root sheath, the inner root sheath (IRS), and the companion layer. Hair follicles are contiguous with the dermal papilla, which is encased by the matrix (4). Postnatal hair follicles progress periodically through three phases: intensive growth and hair shaft formation (anagen), apoptosis-driven regression (catagen) and resting (telogen) (5). The interfollicular epidermis occupies the space between skin appendages and consists of the basal, spinous, granular, and cornified layers. The basal layer, which is mitotically active, commits to cell cycle arrest and terminally differentiates to give rise to the other three layers (6). Recent advances in molecular genetics have led to the identification of many of the genes and pathways that contribute to skin development. Furthermore, mutations in some of these genes are associated with hereditary hair loss disorders (7).

Rhomboid proteins play a significant role in keratinocyte proliferation and wound healing in the skin (8). Specifically, iRhom2 is an inactive member of the rhomboid intramembrane proteinase family and regulates the maturation of TNF-α convertase (TACE, also called ADAM17) (9, 10). In addition, iRhom2 inhibits the release of epidermal growth factor (EGF) family members by binding to EGF ligands in the endoplasmic reticulum (ER), leading to ER-associated degradation in mammals (11). Moreover, the cytoplasmic domain of iRhom2 is involved in regulating the secretion of EGFR ligands and controlling ADAM17-induced shedding (12). Recently, mutations in the N-terminal domain of iRhom2 were reported to cause tylosis esophageal cancer in three human families (13).

To identify differentially expressed proteins in the dorsal skin of homozygous *iRhom2*^{Uncv} and wild-type mice at postnatal day 5 (P5), we performed two-dimensional gel electrophoresis (2-DE) followed by MALDI-TOF-MS (matrix-assisted laser desorption ionization time of flight mass spectrometry). Twelve proteins were identified as being differentially expressed, and some of

*Corresponding authors. Wen-Long Li, Tel: +86-10-66948230; Fax: +86-10-63813969; E-mail: liwl@bmi.ac.cn, Lin Zeng, Tel: +86-10-66948230; Fax: +86-10-63813969; E-mail: neaucn@126.com

http://dx.doi.org/10.5483/BMBRep.2015.48.1.022

Received 24 January 2014, Revised 13 February 2014, Accepted 16 March 2014

Keywords: Hair follicle, iRhom2, Proteomic, Skin, Uncv

ISSN: 1976-670X (electronic edition)

these expression changes were tested and confirmed using quantitative real-time PCR (qRT-PCR), western blot and immunohistochemistry. Our proteomic results indicate that several differentially expressed skin proteins might be involved in the mechanism by which iRhom2 regulates skin development.

RESULTS

The genotyping of homozygous *iRhom2*^{Uncv} mice using PCR

Through the identification of a 309-bp deletion in *iRhom2* of homozygous *iRhom2*^{Uncv} mice, PCR analysis was used to identify the genotype of the mice. A 760-bp fragment was amplified by PCR in wild-type mice, whereas a 451-bp fragment was amplified in homozygous *iRhom2*^{Uncv} mice (Fig. 1A).

Identification of differentially expressed proteins in the skin of wild-type mice and homozygous *iRhom2*^{Uncv} mice

Comparative proteomic approaches were used to analyze differentially expressed skin proteins in wild-type mice and homozygous *iRhom2*^{Uncv} mice. The total skin proteins from mice at P5 were collected and subjected to 2-DE with an isoelectric focusing (IEF) range of pH 3 to 10. To achieve better resolution for protein separation, each protein sample was run on 10% and 12% SDS-PAGE gels. Twelve proteins exhibited significant quantitative and qualitative variances (1.2-fold change and $P < 0.05$). These proteins were identified successfully using MALDI-TOF-MS and then qualified using the Mascot search engine (Table 1). Eight differentially expressed spots were observed in the 10% SDS-polyacrylamide gel, and 4 spots were observed in the 12% SDS-polyacrylamide gel (Fig. 1B). Among them, seven proteins

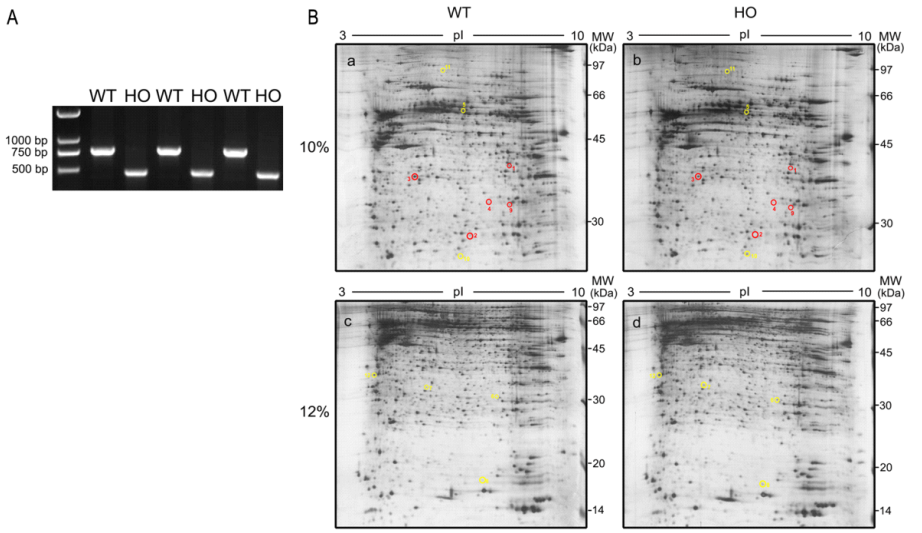

Fig. 1. 2-DE gel separation of skin proteins from homozygous *iRhom2*^{Uncv} and wild-type littermates. (A) Genotyping of homozygous *iRhom2*^{Uncv} mice using PCR. Genomic DNA was extracted from mouse tails and amplified by PCR using specific primers. A 760-bp fragment was amplified from wild-type mice, and a 451-bp fragment was amplified from homozygous *iRhom2*^{Uncv} mice. WT: wild-type at P5, HO: homozygous at P5. (B) Proteins were separated on IPG-strips with pH 3-10 in the first dimension and 10% (a and b) and 12% (c and d) polyacrylamide gel in the second dimension. The gels were stained with CBB. Red circles indicate downregulated spots, and yellow circles indicate upregulated spots. 10%: 10% polyacrylamide gel, 12%: 12% polyacrylamide gel.

Table 1. Upregulated and downregulated proteins in a comparison between wild-type and homozygous *iRhom2*^{Uncv} mice as identified by MS and the spot volume differences

Protein spot#	Protein name	NCBI accession	Peptides matched	Theoretical/observed		Fold change
				pI	MW (kDa)	
1	Heterogeneous nuclear ribonucleoprotein A/B isoform 2	gi|6754222	8 (4)	7.7/7.94	30.8/39.6	−2.00
2	Peroxiredoxin-6	gi|3219774	11 (4)	5.71/6.88	24.8/28.0	−3.13
3	Prohibitin	gi|6679299	25 (15)	5.57/5.36	29.8/37.5	−2.09
4	Keratin73	gi|47059013	2 (1)	8.36/7.37	58.9/33	−2.07
5	Coronin-1	gi|4895037	9 (4)	6.05/6.67	50.9/57.3	1.82
6	PREDICTED: dynein heavy chain 12, axonemal	gi|377833366	2 (0)	7.46	31.9	1.83
7	Protein 40 kD	gi|226005	3 (1)	4.80/5.47	32.7/35.4	2.51
8	Transgelin	gi|5007032	6 (4)	6.59/7.06	23.6/18.4	2.43
9	MEMO1	gi|19526994	10 (3)	6.67/7.94	33.7/32.6	−2.81
10	Peroxiredoxin-1	gi|6754976	3 (2)	8.26/6.63	22.2/26.3	1.73
11	Unnamed protein product	gi|26354755	9 (6)	5.68/6.09	80.7/94.0	2.13
12	Polymerase I and transcript release factor	gi|6679567	15 (8)	5.43/4.34	43.9/35.9	1.87

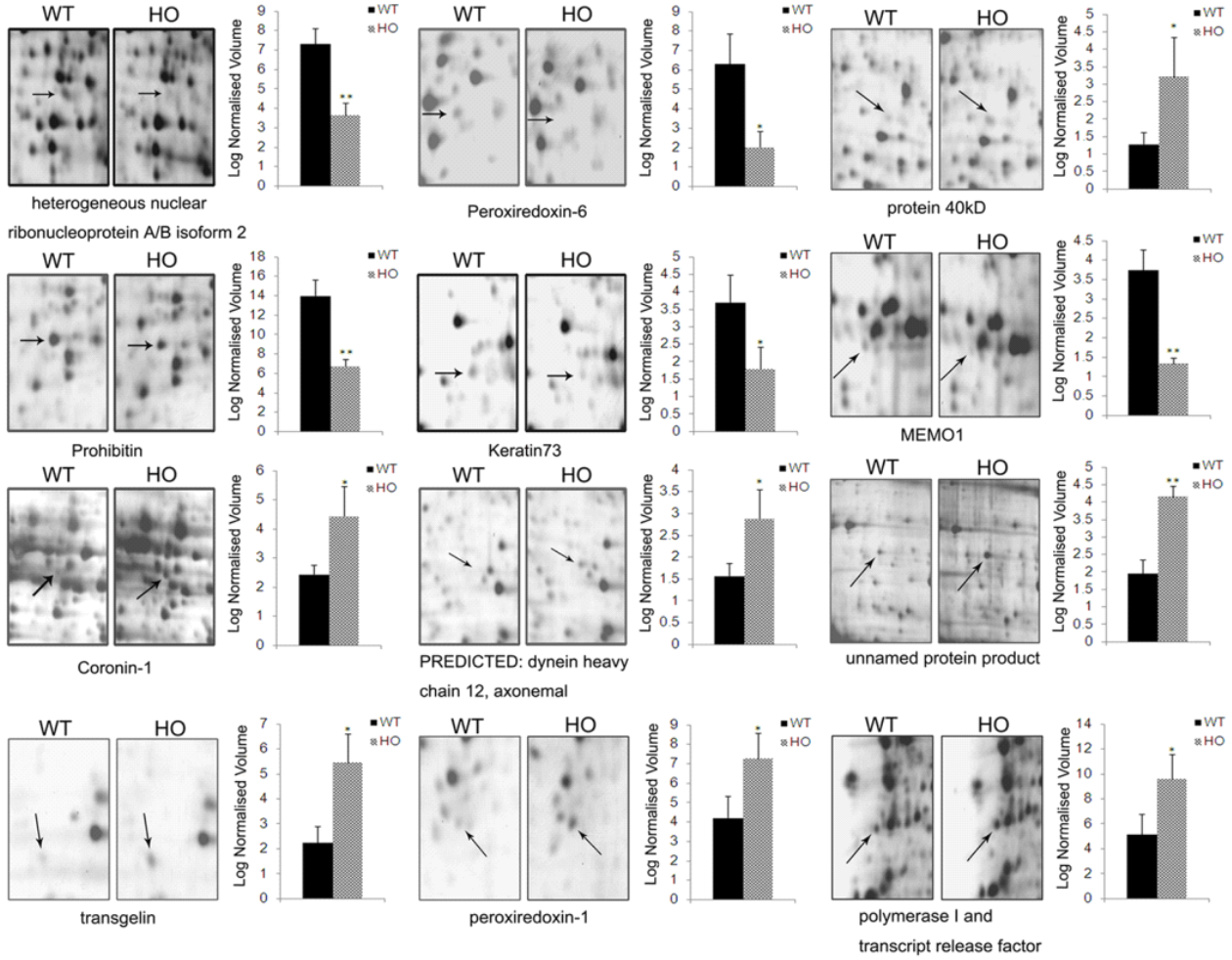

Fig. 2. Close-up of the regions of differentially expressed protein spots and statistical analysis of the normalized spot volumes. Three independent experiments were performed and the mean ± SD was plotted (*P < 0.05, **P < 0.01 compared with wild-type mice).

were upregulated in the skin of homozygous *iRhom2*^{Uncv} mice compared with wild-type mice, including Coronin-1 (Coro-1); PREDICTED: dynein heavy chain 12, axonemal; protein 40 kD; Transgelin; Peroxiredoxin-1; Polymerase I and transcript release factor; and an unnamed protein product (Fig. 2). Five proteins were downregulated, including heterogeneous nuclear ribonucleoprotein A/B isoform 2; Peroxiredoxin-6; Prohibitin (Phb); Keratin73 (KRT73); and Mediator of cell motility 1 (MEMO1) (Fig. 2). KRT73 expression was reduced more than 2-fold in homozygous *iRhom2*^{Uncv} mice (Fig. 2). Coro-1 was upregulated more than 1.8-fold in the skin of homozygous *iRhom2*^{Uncv} mice compared with wild-type mice (Fig. 2). MEMO1 expression was downregulated more than 2.8-fold in the skin of homozygous *iRhom2*^{Uncv} mice compared with wild-type mice (Fig. 2).

Verification of proteomic analysis

To validate the results of our proteomics analysis, we performed qRT-PCR, immunohistochemistry and western blot analysis for several of the identified proteins. The qRT-PCR results showed that *Krt73* was 1.5 times more abundant in the wild-type mice than in the homozygous *iRhom2*^{Uncv} mice at P5 (Fig. 3A). Western blotting confirmed that the expression of KRT73 was dramatically reduced in the skin of homozygous *iRhom2*^{Uncv} mice (Fig. 3B). In the hair follicles of wild-type mice, a large number of KRT73-positive cells were found in the IRS at P5 (Fig. 3C). However, the number of positive cells was significantly reduced in the follicles of homozygous *iRhom2*^{Uncv} mice compared with those of wild-type mice at P5 (Fig. 3C). *Coro-1* was upregulated more than 2-fold in homozygous *iRhom2*^{Uncv} mice at P5 (Fig. 3A). This upregulated expression of Coro-1 in the skin of homozygous *iRhom2*^{Uncv} mice was confirmed by western blot-

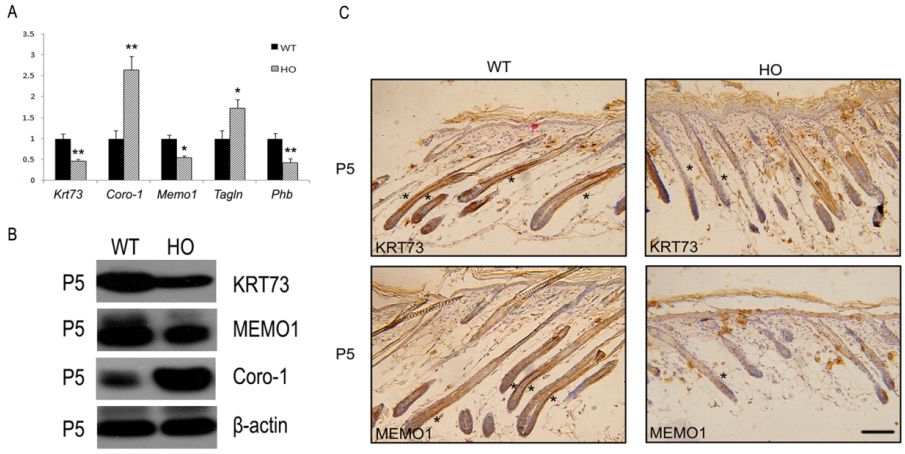

Fig. 3. Verification of proteomic analysis by qRT-PCR and immunohistochemistry analyses. (A) Relative mRNA expression of *Krt73*, *Coro-1*, *Memo1*, *Phb* and *Tagln* in the dorsal skin of wild-type and homozygous *iRhom2*^{Uncv} littermates at P5. Each bar represents the mean ± SD (*P < 0.05, **P < 0.01 compared with wild-type mice). (B) The expression of KRT73, MEMO1 and Coro-1 was detected by western blot using specific antibodies. (C) Immunohistochemical staining of KRT73 and MEMO1 performed on skin sections of P5 wild-type and homozygous *iRhom2*^{Uncv} mice. Scale bars = 50 μm.

ting (Fig. 3B). Memo1 was downregulated more than 1.5-fold in homozygous *iRhom2*^{Uncv} mice at P5 according to qRT-PCR (Fig. 3A). The western blotting results confirmed that the expression of MEMO1 was significantly reduced in the follicles of homozygous *iRhom2*^{Uncv} mice compared with those of wild-type mice (Fig. 3B). The immunohistochemistry results also consistently confirmed that the number of cells positive for MEMO1 was decreased in the skin of homozygous *iRhom2*^{Uncv} mice compared with that of wild-type mice at P5 (Fig. 3C). Phb expression was significantly decreased in homozygous *iRhom2*^{Uncv} mice compared with wild-type mice (Fig. 3A). In addition, the level of the *Tagln* was significantly elevated in homozygous *iRhom2*^{Uncv} mice compared with wild-type mice (Fig. 3A).

DISCUSSION

Proteomic approaches were applied to identify differentially expressed skin proteins in wild-type and homozygous *iRhom2*^{Uncv} littermates at P5. Seven proteins were upregulated in homozygous *iRhom2*^{Uncv} mice compared with wild-type mice, and five proteins were downregulated. Some of these results were independently tested and confirmed using qRT-PCR and immunohistochemistry, demonstrating the reliability of our 2-DE analysis.

The development of hair follicles in murine dorsal skin is completed at P6.5-P7.5 (anagen), the hair shaft is produced until P14.5-P16.5, and the hair follicles then enter catagen (16). Therefore, proteins differentially expressed during hair morphogenesis before P6.5 are significant when analyzing the mechanism by which the hairless phenotype develops in homozygous *iRhom2*^{Uncv} mice. This was why mouse littermates at P5 were selected to carry out proteomic analysis of skin protein expression.

During the differentiation of hair follicles, keratins containing type I and type II proteins are expressed in highly specific patterns associated with the epithelial type and stage of cellular differentiation (17). KRT73 is a type II keratin protein that is specifically expressed in the IRS cuticle (14). In addition, the expression of KRT73 in the IRS cuticle initiates approximately in the lowermost bulb region and ends in a region of terminal differentiation of the IRS cuticle cells, which is equivalent to the uppermost cortex region (18). The proteomic results revealed the downregulation of KRT73 in homozygous *iRhom2*^{Uncv} mice, suggesting a possible defect in the IRS cuticle. Decreased numbers of KRT73-positive cells were also observed in the IRS of homozygous *iRhom2*^{Uncv} mice, further confirming that the follicle IRS of homozygous *iRhom2*^{Uncv} mice was abnormally differentiated.

Coro-1 was significantly upregulated in the skin of homozygous *iRhom2*^{Uncv} mice compared with that of wild-type mice. Coro-1 is required to control the activation of calcium signaling, sustaining the survival of naive T cells and promoting the escape of pathogenic *M. tuberculosis* from lysosomal degradation in macrophages (19). Therefore, the overexpression of Coro-1 in the skin of homozygous *iRhom2*^{Uncv} mice suggests a possible inflammatory reaction in this organ, but further experiments are required to confirm this finding.

Notably, MEMO1 expression was significantly downregulated in homozygous *iRhom2*^{Uncv} mice. MEMO1, a 297 amino-acid protein, is involved in ErbB2-induced breast carcinoma cell motility (20). In addition, MEMO1 induces the epithelial–mesenchymal transition, which is required for early embryogenesis (21). Interestingly, Memo1 conditional-knockout mice display graying hair and alopecia (22). Consistent with this, the downregulation of MEMO1 in homozygous *iRhom2*^{Uncv} mice indicates that MEMO1 might play a vital role in iRhom2-mediated skin development.

This research is a proteomics-based study that identifies key upregulated and downregulated skin proteins that contribute to the iRhom2-mediated regulation of skin development. Although the detailed functions of these genes in skin development remain to be determined, their identification, especially KRT73, MEMO1 and Coro-1, will serve as helpful resources when studying the molecular mechanisms through which iRhom2 regulates skin development.

MATERIALS AND METHODS

Animals

Homozygous *iRhom2*^{Uncv} and wild-type littermates in the BALB/c genetic background were produced by intercrossing heterozygote *iRhom2*^{Uncv} mice. The offspring were genotyped using PCR analysis of genomic DNA isolated from the tail. The PCR protocol consisted of 30 cycles of 94°C for 30 s, 60°C for 30 s and 72°C for 30 s. The following genotyping primers were used: *iRhom2* forward (fwd), 5′-ATGTACCTTCGCCCTCACCTCC-3′ and reverse (rev), 5′-CCCCACCACTTCTCCCATAACC-3′. A 760-bp fragment was amplified from wild-type mice, and a 451-bp fragment was amplified from homozygous *iRhom2*^{Uncv} mice. The animal work was performed following a protocol approved by the Institute of JingFeng Medical Laboratory Animal, Beijing, China.

Preparation of skin protein samples

Dorsal skin samples were obtained from three groups of wild-type and homozygous *iRhom2*^{Uncv} littermates at P5 to compare skin protein expression. The skin tissues were ground to a fine powder using a liquid nitrogen mortar and dissolved in lysis buffer (protease inhibitor cocktail [Roche Diagnostic, Mannheim, Germany], 40 mM Tris, 0.1 mg/ml RNase A, 1 mM EDTA, 7 M urea, 1% dithiothreitol [DTT], 0.1 mg/ml DNase, 2 M thiourea and 4% CHAPS). After centrifugation twice at 12,000 g for 30 min at 4°C, the supernatant was collected. The protein concentration was determined using the Bio-Rad Protein Assay (Bio-Rad, Hercules, CA, USA) according to the manufacturer's instructions.

Two-dimensional gel electrophoresis and image analysis

A 160 μg sample of skin protein was diluted with rehydration buffer (8 M urea, 0.5% IPG buffer [Amersham Pharmacia Biotech, Sweden] and 4% CHAPS) and separated using IEF on 18 cm (pH 3-10) linear Immobiline Dry Strips (Amersham Pharmacia Biotech, Sweden). The strips were subjected to IEF according to the manufacturer's suggested protocol using the IPGphor system (Amersham Pharmacia Biotech, Sweden). The second dimension was performed on a Protean II Cell (Bio-Rad) using 10% and 12% SDS-polyacrylamide gels, which were stained with Coomassie Brilliant Blue (CBB). The 2-DE images were scanned with an Image Scanner (Amersham Pharmacia Biotech, Sweden), and the gel images were analyzed using ImageMaster 2D software (Amersham Pharmacia Biotech, Sweden). The individual protein spot volumes were normalized relative to the detected total spot volume. Spots with significantly different (P value < 0.05) normalized volumes (fold-change ≥ 1.5) were identified using MS.

In-gel digestion and MS identification

Differentially expressed gel spots were selected to digest as previously described (23). The protein peptides were analyzed using Bruker Reflex III MALDI-TOF-MS (Bruker-Franzen, Germany). Monoisotopic peptide masses were used for database searches, allowing a 100 ppm mass accuracy and one missed cleavage. Cysteine carbamidomethylation and methionine oxidation were considered. The proteins were identified by peptide mass fingerprinting using the Mascot search engine (http://www.matrixscience.com, Matrix Science, London, UK) against the Swiss-Prot and NCBInr databases.

RNA isolation and qRT-PCR

The dorsal skin of wild-type mice and homozygous *iRhom2*^{Uncv} mice at P5 was harvested. Total RNA was isolated from the skin using TRIzol reagent (Invitrogen, USA) according to the manufacturer's protocol. First strand cDNA was synthesized from total RNA using the Prime Script RT reagent kit (TaKaRa, Japan) with oligo-dT primers according to the manufacturer's protocol. qRT-PCR was performed in triplicate using SYBR Premix Ex Taq (TaKaRa). The gene expression levels were normalized to *GAPDH* and calculated using the $\Delta\Delta$cycle threshold method. The following primers were used to amplify the indicated genes: *Keratin73* (*Krt73*) fwd, 5′-CCTGGAGTTGCCAACAGGG-3′ and rev, 5′-CTGCCCGGTAAGAGGATGAG-3′; *Coronin-1* (*Coro-1*) fwd, 5′-TGGCTCTGATCTGTGAGGC-3′ and rev, 5′-TCTTGTCTACTCGTCCAGTCTTG-3′; *Mediator of cell motility 1* (*Memo1*) fwd, 5′-GGATACACATACTGTGGGTCCT-3′ and rev, 5′-CAGGGGCACATGATGGGAAG-3′; *Prohibitin* (*Phb*) fwd, 5′-GATTCCGTGGCGTACAGGAC-3′ and rev, 5′-GCGGCAGTCAAAGATAATTGGTT-3′; *Transgelin* (*Tagln*) fwd, 5′-CCAACAAGGGTCCATCCTACG-3′ and rev, 5′-ATCTGGGCGGCCTACATCA-3′; and GAPDH fwd, 5′-AAATGGTGAAGGTCGGTGTG-3′ and rev, 5′-TGAAGGGGTCGTTGATGG-3′.

Immunohistochemistry analysis

Dorsal skin tissue samples were fixed in 4% paraformaldehyde at 4°C overnight, embedded in paraffin and sectioned at 4 μm. The immunoreactivity of antigens was heat-restored using citrate buffer (pH 6). To block the endogenous peroxidase activity of the skin, the sections were blocked in 10% goat serum, treated with 0.3% H_2O_2 and rinsed with PBS. Primary antibodies against the following proteins were used: KRT73 (Abcam, UK; 1:10), MEMO1 (Abcam, UK; 1:200), and Coro-1 (Abcam, UK; 1:100). The bound antibodies were detected using diaminobenzidine, and the sections were counterstained with hematoxylin. Images of the tissue sections were analyzed using a fluorescence microscope (BX51; Olympus, NY) equipped with a cooled CCD camera system (DP-72; Olympus, NY).

Western blot analysis

Total protein extracted from skin tissue was separated using 10% SDS-gel electrophoresis and subsequently transferred to PVDF (Millipore) using a Mini Trans-Blot Cell (BioRad). The membrane was incubated with the following primary antibodies: KRT73 (Abcam, UK; 1:100), MEMO1 (Abcam, UK; 1:1000), and Coro-1 (Abcam, UK; 1:250). An anti-β-actin (Abcam, UK; 1:5000) antibody served as a control. The membrane was then incubated with an HRP-conjugated secondary antibody. Proteins were detected using an ECL kit.

Statistical analysis

The data are expressed as the mean ± standard deviation (SD) of three independent experiments. Statistical significance between the wild-type and homozygous *iRhom2*^{Uncv} mice was determined using Student's t-test. A P value < 0.05 was considered statistically significant.

ACKNOWLEDGEMENTS

We would like to express our appreciation to Hong-Li Wang and Feng Liu for their technical advice and practical assistance. Mass spectrometry was conducted at the National Center of Biomedical Analysis of China. This project was supported by the National Natural Science Foundation of China (31030058).

REFERENCES

1. Li SR, Wang DP, Yu XL et al (1999) Uncv (uncovered): a new mutation causing hairloss on mouse chromosome 11. Genet Res 73, 233-238
2. Shi YZ, Wang DP, Hu LD et al (2003) A high-resolution genetic and physical map of a mouse coat abnormality locus (Uncv). Sheng Wu Hua Xue Yu Sheng Wu Wu Li Xue Bao (Shanghai) 35, 397-402
3. Fuchs E (2007) Scratching the surface of skin development. Nature 445, 834-842
4. Legue E, Sequeira I and Nicolas JF (2010) Hair follicle renewal: authentic morphogenesis that depends on a complex progression of stem cell lineages. Development 137, 569-577
5. Alonso L and Fuchs E (2006) The hair cycle. J Cell Sci 119, 391-393
6. Nagarajan P, Romano RA and Sinha S (2008) Transcriptional control of the differentiation program of interfollicular epidermal keratinocytes. Crit Rev Eukaryot Gene Expr 18, 57-79
7. Nakamura M, Schneider MR, Schmidt-Ullrich R and Paus R (2013) Mutant laboratory mice with abnormalities in hair follicle morphogenesis, cycling, and/or structure: an update. J Dermatol Sci 69, 6-29
8. Etheridge SL, Brooke MA, Kelsell DP and Blaydon DC (2013) Rhomboid proteins: a role in keratinocyte proliferation and cancer. Cell Tissue Res 351, 301-307
9. Adrain C, Zettl M, Christova Y, Taylor N and Freeman M (2012) Tumor necrosis factor signaling requires iRhom2 to promote trafficking and activation of TACE. Science 335, 225-228
10. McIlwain DR, Lang PA, Maretzky T et al (2012) iRhom2 regulation of TACE controls TNF-mediated protection against Listeria and responses to LPS. Science 335, 229-232
11. Zettl M, Adrain C, Strisovsky K, Lastun V and Freeman M (2011) Rhomboid family pseudoproteases use the ER quality control machinery to regulate intercellular signaling. Cell 145, 79-91
12. Maretzky T, McIlwain DR, Issuree PD et al (2013) iRhom2 controls the substrate selectivity of stimulated ADAM17-dependent ectodomain shedding. Proc Natl Acad Sci U S A 110, 11433-11438
13. Blaydon DC, Etheridge SL, Risk JM et al (2012) RHBDF2 mutations are associated with tylosis, a familial esophageal cancer syndrome. Am J Hum Genet 90, 340-346
14. Porter RM, Corden LD, Lunny DP, Smith FJ, Lane EB and McLean WH (2001) Keratin K6irs is specific to the inner root sheath of hair follicles in mice and humans. Br J Dermatol 145, 558-568
15. Langbein L, Rogers MA, Praetzel-Wunder S, Helmke B, Schirmacher P and Schweizer J (2006) K25 (K25irs1), K26 (K25irs2), K27 (K25irs3), and K28 (K25irs4) represent the type I inner root sheath keratins of the human hair follicle. J Invest Dermatol 126, 2377-2386
16. Botchkarev VA and Paus R (2003) Molecular biology of hair morphogenesis: development and cycling. J Exp Zool B Mol Dev Evol 298, 164-180
17. Langbein L and Schweizer J (2005) Keratins of the human hair follicle. Int Rev Cytol 243, 1-78
18. Langbein L, Rogers MA, Praetzel S, Winter H and Schweizer J (2003) K6irs1, K6irs2, K6irs3, and K6irs4 represent the inner-root-sheath-specific type II epithelial keratins of the human hair follicle. J Invest Dermatol 120, 512-522
19. Pieters J, Muller P and Jayachandran R (2013) On guard: coronin proteins in innate and adaptive immunity. Nat Rev Immunol 13, 510-518
20. Marone R, Hess D, Dankort D, Muller WJ, Hynes NE and Badache A (2004) Memo mediates ErbB2-driven cell motility. Nat Cell Biol 6, 515-522
21. Sorokin AV and Chen J (2013) MEMO1, a new IRS1-interacting protein, induces epithelial-mesenchymal transition in mammary epithelial cells. Oncogene 32, 3130-3138
22. Haenzi B, Bonny O, Masson R et al (2013) Loss of Memo, a novel FGFR regulator, results in reduced lifespan. FASEB J 28, 327-336
23. Cui JW, Wang J, He K et al (2005) Two-dimensional electrophoresis protein profiling as an analytical tool for human acute leukemia classification. Electrophoresis 26, 268-279